The current issue and full text archive of this journal is available at
www.emeraldinsight.com/0961-5539.htm

Numerical modelling of a vapour bubble growth in uniformly superheated liquid

Y.Y. Yan
School of the Built Environment, University of Nottingham, University Park, UK, and
W.Z. Li
Department of Power Engineering, Dalian University of Technology, Dalian City, China

Abstract

Purpose – The paper aims at studying numerically a vapour bubble growth in uniformly superheated liquid.

Design/methodology/approach – Time dependent mathematical and numerical models are developed. Based on the Stefan boundary condition, the rate of heat transfer at the vapour-liquid interface and the rate of bubble growth are calculated.

Findings – It is found that, at the initial stage of bubble growth, both the growth rate and the mean Nusselt number at bubble interface have the maximum values, then they decrease with time; the rate of bubble growth also has a significant effect on bubble deformation; the growth tends to keep the bubble at its initial shape. In addition, the growth and deformation of a vapour bubble have much influence on temperature propagation in the vicinity of the bubble-liquid interface; the temperature wake at the rear of the bubble occurs at high Reynolds number but does not appear at low Reynolds number.

Originality/value – The paper is based on the authors' original work, focusing on the behaviour of a vapour bubble in uniformly superheated liquid–an issue of importance in the field of boiling and two phase flow.

Keywords Vapours, Modelling, Numerical analysis

Paper type Research paper

Nomenclature

C_b	= constant, see equation (2)	t	= time, dimensionless time
d_e	= bubble equivalent diameter	T	= Temperature
h_{fg}	= specific heat capacity of evaporation	T_∞	= The temperature of liquid at the terminal boundary of bubble growth
J	= a determinant value of metric tensor		
p	= pressure	u	= Cartesian velocity component in x-direction
r	= coordinate		
R_b	= curvature radius of vapour bubble	v	= Cartesian velocity component in r-direction
Re	= Reynolds number ($= \rho U_T d_e/\mu$)		
S	= bubble surface area	U	= contravariant velocity component
S_ϕ	= source term in general governing equation, equation (1)	U_T	= bubble terminal rising velocity
		V	= contravariant velocity component

International Journal of Numerical Methods for Heat & Fluid Flow
Vol. 16 No. 7, 2006
pp. 764-778
© Emerald Group Publishing Limited
0961-5539
DOI 10.1108/09615530610683502

The authors wish to acknowledge support for this work by the National Nature Science Foundation of China (50476074) and the UK EPSRC under grant GR/M90207.

V_b = bubble volume
We = Weber number (= $\rho U_T U_T d_e/\sigma$)
x = coordinate

Greek symbols
α = covariant metric tensor
δ = difference operator
ϕ = general dependent variable
γ = covariant metric tensor
η = coordinate in computational space
μ = dynamic viscosity
ρ = density
σ = surface tension
τ = shear stress
ξ = coordinate in computational space
Δ = gradient operator
Γ = diffusion coefficient
$\Re$ = ratio of bubble volume at the present step to the last

Subscripts
b = values at the interface
$b-1$ = values on the point one grid away from the interface
e = equivalent
g = grid
o = values of the gas inside bubble, initial state
τ = tangential direction

Superscripts
n = values at the last iteration step
p = values at the predictor phase
$n+1$ = values at the present iteration step

Introduction

The behaviour of a vapour bubble in uniformly superheated liquid is of fundamental importance in the field of boiling and two-phase flow. Boiling occurs when the temperature of the heater surface exceeds the saturated temperature, thus causing bubble formation at nucleate centres; and at a certain condition, the nucleate bubbles will departure from the heater wall. If the temperature of bulk liquid is above saturation, the vapour bubbles will grow in the liquid; the analogue process is bubble collapse. Such behaviour of bubble is often influenced by temperature and velocity gradients and the balance of surface tension forces at liquid-gas interface. Moreover, predicting vapour bubble behaviour in superheated liquid is an important step in modelling void growth, bubble dynamics and boiling heat transfer of flow boiling, which have many applications in the power, refrigeration and chemical and process industries.

In the past few years, problems of unsteady deformations of inert bubbles excluding bubble growth, which are important for understanding bubble behaviour in non-boiling reactors or systems, have been studied by several researchers; these have been reviewed and reported by Clift *et al.* (1978), Magnaudet and Eames (2000), Yan and Li (2002) and Yan *et al.* (2002), respectively. Such problems of bubble deformation are often regarded as pure free surface flow problems of fluid dynamics. It is assumed that the change of interfacial stresses acting on the surface of a bubble results in a deformation of the bubble when it rises freely through an unbounded quiescent liquid; meanwhile, the deformation of bubble is also dependent on the characteristics of fluid flow around it, while, such characteristics is actually also resulted from the change of bubble shape. In many practical applications, heat and mass transfer always take place when a bubble rises in a hot liquid. Typically, for a vapour bubble, if the temperature of the liquid exceeds its saturated temperature, a phase change will take place at the vapour-liquid interface and the vapour bubble will grow when it rises in the liquid.

The problems concerned with vapour bubble growth are often more complicated. The deformation of a vapour bubble in superheated liquid is not only because of the change of stress forces acted on the interface as fluid flowing around the bubble but also because of the volume increase of the vapour bubble when a phase change takes place at the

interface. The co-actions and interactions between the vapour-liquid interface and the surrounding bulk liquid constitute a complicated moving boundary problem accompanying with heat and mass transfer; meanwhile, the movement of the interface needs to be calculated as a part of the solution for continuity, momentum and energy equations. In addition, the analogous problem of vapour bubble growth is of bubble collapse, which is also a popular physical phenomenon. Early studies on vapour bubble dynamics were based on the Rayleigh equation and its modification, which were basically dealing with zero or one dimensional problems (Plesset and Zwick, 1953). Wittke and Chao (1967) studied the collapse of a spherical bubble with translatory motion; but the deformation of the bubble was not considered in their work. Cao and Christensen (2000) simulated the bubble collapse in a binary solution; where the Navier-Stokes equation was transformed in terms of the stream function and vorticity method in two-dimensional axisymmetric moving non-orthogonal body-fitted coordinates. Han *et al.* (2001) used a mesh-free method to simulate bubble deformation and growth in nucleate boiling, but the flow fields were considered as a pure two-dimensional problem, a bubble's three-dimensional nature might have been ignored. Fujita and Bai (1998) using arbitrary Lagrangian-Eulerian (ALE) method simulated the growth of a single bubble attached at a horizontal surface with a constant contact angle before its departure; but a non-slip condition was applied to the vapour-liquid boundary, the tangential flow along the interface was not considered. Son and Dhir (1998) also calculated the growth of a single bubble during partial nucleate boiling on a horizontal surface by the level-set method, but the details of physical messages of flow fields in the vicinity of the interface were not supplied. Other two notable works on vapour bubble growth and dynamics include Buyevich and Webbon (1996) and Mei *et al.* (1995a,b); in which bubble dynamics typically the microlayer analysis has been carried out; but in their works, numerical strategies have not been intensively discussed. Nevertheless, except the above papers which are relevant to the present work, little information is reported about the vapour bubbles deformation and growth in superheated liquid. In particular, few papers have been reported on propagations of temperature fields around a growing and deforming vapour bubble.

The aim of this paper is to develop the methodology for predicting bubble deformation and temperature field propagation induced by phase change at the interface of a growing vapour bubble in superheated liquid. Time dependent physical and mathematical models and according numerical procedures are developed. Based on this, numerical simulations are carried out.

Numerical methods

Assumptions

In order to address the behaviour of a vapour bubble in uniformly superheated liquid, the following assumptions are considered:

- The surface tension coefficient of vapour-liquid interface is a constant; surface tension forces only change with angle of surface circumference.
- The flow and temperature fields around the bubble are axisymmetric.
- The hot liquid is unbounded quiescent incompressible Newtonian fluid. The rising span of vapour bubble is so short that the hydrodynamics pressure acted on the interface can be considered as a constant.

- The vapour inside bubble is pure and incompressible; the heat transferred from the liquid to the interface is completely used to evaporate the liquid at the interface, this results in the net increase of bubble volume.
- The temperature inside the vapour bubble is uniform, so that the temperature gradient is zero.
- The thermal properties for both the vapour and liquid are constant.

Governing equation and discretisation

The numerical method applied is based on a velocity-pressure formulation combined with a finite-volume discretisation of the Navier-Stokes equations written in a non-orthogonal body-fitted coordinate (BFC) of ($\xi\ \eta\ \theta$); where θ is the azimuthal angle, measured about the axis of symmetry. With the assumption of axisymmetry, the coordinates can be connected with the common cylindrical coordinates of ($x,\ r,\ \theta$) as shown in Figure 1 and the corresponding domain is also shown in the figure; where curvilinear line of that $\xi = 0$ fits the interface of gas-liquid. With respect to the ($\xi\ \eta$) system, the mapping is always defined in such a way that the solution domain is defined by $0 \leq \xi \leq 1$ and $0 \leq \eta \leq 1$. A further reference for using non-orthogonal body-fitted BFC to solve Navier-Stokes equations can be found in authors other works (Yan and Li, 2002; Li and Yan, 2002a, b). In the present modelling, Cartesian velocity components (u, v) are employed as dependent variables to predict the flow and heat and mass transfer at the interface. For the study of time-dependent bubble deformation, the moving boundary is employed and solved as a part of solution for continuity, momentum and energy equations, in which the velocities in convection term of the governing equations are replaced by relative velocities U_r and V_r. The conservation equations for a general dependent variable ϕ in the non-orthogonal coordinate system (ξ, η) take the following general form:

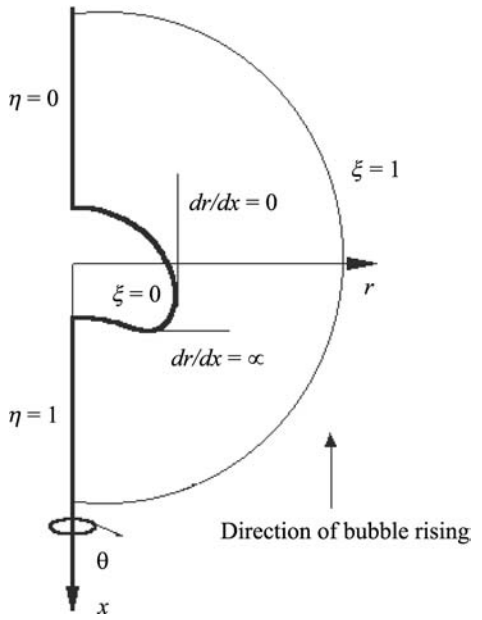

Figure 1.
The coordinate system and domain

$$\frac{\partial \rho J \phi}{\partial t} + \frac{\partial}{\partial \xi} r\left[\rho U_{\mathrm{r}} \phi - \frac{\Gamma}{J}\left(\alpha \frac{\partial \phi}{\partial \xi} - \beta \frac{\partial \phi}{\partial \eta}\right)\right] + \frac{\partial}{\partial \eta} r\left[\rho V_{\mathrm{r}} \phi - \frac{\Gamma}{J}\left(-\beta \frac{\partial \phi}{\partial \xi} + \gamma \frac{\partial \phi}{\partial \eta}\right)\right] = rJS_{\phi}(\xi, \eta) \tag{1}$$

where:

$$U_{\mathrm{r}} = (u - u_{\mathrm{g}})\frac{\partial r}{\partial \eta} - (v - v_{\mathrm{g}})\frac{\partial x}{\partial \eta},$$

$$V_{\mathrm{r}} = (v - v_{\mathrm{g}})\frac{\partial x}{\partial \xi} - (u - u_{\mathrm{g}})\frac{\partial r}{\partial \xi}$$

$$\alpha = \left(\frac{\partial x}{\partial \eta}\right)^2 + \left(\frac{\partial r}{\partial \eta}\right)^2,$$

$$\beta = \frac{\partial x}{\partial \xi}\frac{\partial x}{\partial \eta} + \frac{\partial r}{\partial \xi}\frac{\partial r}{\partial \eta},$$

$$\gamma = \left(\frac{\partial x}{\partial \xi}\right)^2 + \left(\frac{\partial r}{\partial \xi}\right)^2,$$

and

$$J = \frac{\partial x}{\partial \xi}\frac{\partial r}{\partial \eta} - \frac{\partial x}{\partial \eta}\frac{\partial r}{\partial \xi}.$$

In the above equations, $S_{\phi}(\xi, \eta)$ is the source of ϕ in $(\xi\,\eta)$ coordinates, U_{r} and V_{r} are relative contravariant velocity components which are particularly defined for the problem of time-dependent bubble deformation; $(u_{\mathrm{g}}, v_{\mathrm{g}})$ are grid velocity components in Cartesian coordinates; α, β and γ are coordinate transformation parameters; J is determinant value of metric tensor; and Γ represents diffusion coefficients.

The finite-volume method is applied to discretise the governing equations. With a staggered grid arrangement, scalar quantities are located at the geometric centre of the control volume and velocity components are displaced in two coordinate directions to lie at the midpoints of control-volume faces.

Terminal shape of bubble growth

Two stages of predicting the terminal shape of a deformable bubble are applied. At the first stage, the outline of a bubble profile, which is described by the position of (x_b^p, r_b^p), is calculated by the following equations:

$$x_b^p = x_b^n - \frac{C_{\mathrm{b}}\Delta P}{\sqrt{\gamma_b}}\left(\frac{\partial r}{\partial \xi}\right)_b \quad \text{and} \quad r_b^p = r_b^n + \frac{C_{\mathrm{b}}\Delta P}{\sqrt{\gamma_b}}\left(\frac{\partial x}{\partial \xi}\right)_b \tag{2}$$

where the last terms in (2) are the components of the normal displacement in x-direction and r-direction; C_{b} is a constant coefficient; the terms of:

$$-\left(\frac{\partial r}{\partial \xi}\right)_b \Big/ \sqrt{\gamma_b} \quad \text{and} \quad \left(\frac{\partial x}{\partial \xi}\right)_b \Big/ \sqrt{\gamma_b}$$

are the direction cosines of normal direction of the interface profile; ΔP is the imbalance total normal stress which is expressed as:

$$\Delta P = p_0 - p + \frac{2}{\gamma J Re}\left(\gamma\frac{\partial V_r}{\partial \eta} - \beta\frac{\partial V_r}{\partial \xi}\right) - \frac{1}{We\sqrt{\gamma}}\left[\frac{1}{\gamma}\left(\frac{\partial r}{\partial \xi}\frac{\partial^2 x}{\partial \xi^2} - \frac{\partial x}{\partial \xi}\frac{\partial^2 r}{\partial \xi^2}\right) + \frac{1}{r}\right] \quad (3)$$

where Re and We are defined by the terminal velocity U_r for $\xi = 1$. The second stage of the prediction is a correction step to determine exact positions of the terminal shape. At a new iteration step, an improved position of the interface is determined as:

$$x_b^{n+1} = \Re x_b^p \quad \text{and} \quad r_b^{n+1} = \Re r_b^p \quad (4)$$

where $\Re$ is a ratio of the old volume to new volume of bubble and expressed as:

$$\Re = \left(\frac{V_b}{V_b + \Delta V_b}\right)^{1/3}, \quad \text{where} \quad V_b = \int_0^1 \pi r^2 \frac{\partial x}{\partial \xi} d\xi. \quad (5)$$

Bubble growth rate

When a vapour bubble of volume V_b, is introduced into superheated liquid, as shown Figure 2. With a time increase of Δt to $t + \Delta t$, the bubble volume is changed to $V_b + \Delta V_b$, as a result of heat and mass transfer. According to the Stefan boundary condition, the heat is transferred from a superheated liquid around the bubble. Based on the assumptions, this heat is completely released and used to change the liquid at interface to vapour added into the bubble so that the volume of the vapour bubble increases accordingly. Thus, the energy conservation equation at the interface can be expressed as:

$$\rho_v h_{fg}\frac{dR_b}{dt} = -\lambda_l\left(\frac{\partial T}{\partial n}\right)_S, \quad (R_b = r|_{\xi=0}); \quad (6)$$

where ρ_v is vapour density, h_{fg} the specific heat capacity of evaporation, λ_l the thermal conductivity of liquid and R_b is the curvature radius of vapour bubble. The equation shows the relationship between the local normal velocity dR_b/dt and the local temperature gradient at the interface. The temperature gradient is a function of fluid property and time-dependent flow field; while the flow field is dependent on bubble deformation. The temperature field is therefore a major driving force for bubble growth or deformation.

Equation (6) is normalized by the followings:

$$\bar{R}_b = \frac{R_b}{d_e}, \quad \bar{t} = \frac{tU_T}{d_e}, \quad \vartheta = \frac{T - T_\infty}{T_b - T_\infty}, \text{and} \quad \bar{n} = \frac{n}{d_e} \quad (7)$$

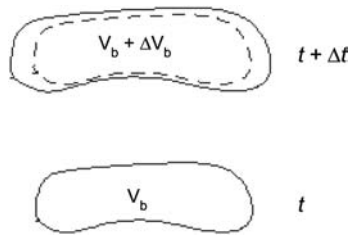

Figure 2.
The growth of a bubble

where d_e is the equivalent diameter of bubble. So, the dimensionless version of equation (6) is obtained as:

$$\frac{d\bar{R}_b}{d\bar{t}} = -\frac{\lambda_l(T_b - T_\infty)}{\rho_v h_{fg} d_e U_T}\left(\frac{\partial \vartheta}{\partial \bar{n}}\right)_S \tag{8}$$

By introducing the Jacob number:

$$Ja = \frac{\rho_l c_{pl}(T_b - T_\infty)}{\rho_v h_{fg}} \tag{9}$$

where c_{pl} is the heat capacity of liquid. Thus, equation (8) can be expressed as:

$$\frac{d\bar{R}_b}{d\bar{t}} = -\frac{Ja}{RePr}\left(\frac{\partial \vartheta}{\partial n}\right)_S \tag{10}$$

This equation shows that the local normal velocity is dependent on the local temperature gradient at the interface. It can be used to determine the local normal displacement resulted from the phase change taken place at the interface. If integrating equation (6) over the area of the bubble surface, the total energy conservation for the bubble can be expressed as:

$$\rho_v h_{fg}\frac{dV_b}{dt} = -\int_S \lambda_l\left(\frac{\partial T}{\partial n}\right)_b dS \tag{11}$$

where V_b is the bubble volume, S the area of bubble surface closing the volume V_b, and dV_b/dt bubble growth rate. Equation (11) can be used to determine the change rate of total volume of the bubble. Similarly, equation (11) can be normalized by using the relations defined in equation (7), and combining the following equations:

$$\bar{V}_b = \frac{V_b}{V_{b0}}, \quad \bar{S} = \frac{S}{S_0} \quad \text{and} \quad \bar{t} = \frac{tU_T}{d_e} \tag{12}$$

where V_{b0} and S_0 are the volume and surface area of the bubble at an initial stage, respectively. So that the dimensionless version of equation (11) can be written as

$$\frac{d\bar{V}_b}{d\bar{t}} = -\frac{6Ja}{RePr}\int_{\bar{S}}\left(\frac{\partial \vartheta}{\partial \bar{n}}\right)d\bar{S} \tag{13}$$

Equation (13) is an expression of determining the change rate of bubble volume, and it is called bubble growth rate in this study. The time term of the equation can be integrated over the dimensionless time interval of $\Delta\bar{t}$ using a full implicit differencing scheme, and the term on the right-hand side of the equation is integrated by numerical integration, so that the discretisation form is given by:

$$\bar{V}_b^{n+1} - \bar{V}_b^n = -\frac{6Ja\Delta\bar{t}}{RePr}\sum_i^{ni}\left(\frac{\partial \vartheta}{\partial \bar{n}}\right)_{b,i}\Delta\bar{S}_i. \tag{14}$$

This equation is used to predict the volume change of a vapour bubble in a hot liquid. On the above basis, the mean Nusselt number at the bubble interface is defined as:

$$Nu_S = \frac{1}{\bar{S}} \sum_{i}^{M} \left(\frac{\partial \vartheta}{\partial \bar{n}} \right)_i \Delta \bar{S}_i. \tag{15}$$

For simplicity and clarity of the notation, the top bar for the above dimensionless parameters will be omitted in the later presentations of the numerical results.

The application of "space conservation law" (SCL)

For flow problems with time dependent moving boundaries, it is necessary to employ the SCL (Demirdzic and Peric, 1988). In mathematics, the SCL can be obtained from equation (1) by setting $\phi = 1$, $\Gamma = 0$, $S(\xi,\eta) = 0$ and $(u,v) = 0$, and this results in:

$$\frac{\partial J}{\partial t} = \frac{\partial}{\partial \xi} \left(u_g \frac{\partial r}{\partial \eta} - v_g \frac{\partial x}{\partial \eta} \right) + \frac{\partial}{\partial \eta} \left(v_g \frac{\partial x}{\partial \xi} - u_g \frac{\partial r}{\partial \xi} \right). \tag{16}$$

Equation (16) implies that the time derivative of the computational cell volume is closely related to the grid velocity. To satisfy the SCL, the grid velocities can be calculated by the definitions of U_r and V_r in equation (1), and the metric tensor J can be updated through equation (16). The final discretised form of equation (16) is solved by applying the SIMPLE algorithm (Patankar, 1980).

Numerical procedures

To predict the deformation of a growing vapour bubble, the transport equations are solved by iteration procedures and appropriate boundary conditions. The numerical procedure proposed is summarised as follows:

(1) assume an initial shape of bubble, for example, spherical, being at rest in stagnant hot liquid.

(2) Generate a non-orthogonal grid to match the bubble shape.

(3) Obtain convergence solutions for the discretised transport equations based on equation (1) by using the SIMPLE algorithm [12].

(4) Move the grid point on the bubble surface by using equation (11) combining the calculation of equations (2)-(5) at a new time step.

(5) Generate a new grid, calculate grid velocities at all nodes and applying the SCL to update the determinant value of metric tensor to guarantee a basic requirement for space conservation.

(6) Repeat (3) ~ (5) until all equations and boundary conditions are satisfied.

Results and discussion

The time scales applied in all calculations of this paper are dimensionless; but to simplify the representation the top bar of $\bar{t}$ is omitted and expressed as t in the Figures 2-7.

Bubble growth rate and heat transfer

The growth rate of vapour bubble defined by equation (13) and the mean Nusselt number at bubble interface are calculated using the method developed in this paper. Four cases for (Re, We) = (2,20), (Re, We) = (*20,15*), (Re, We) = (100,6) and (Re, We) = (200,4) are calculated, respectively.

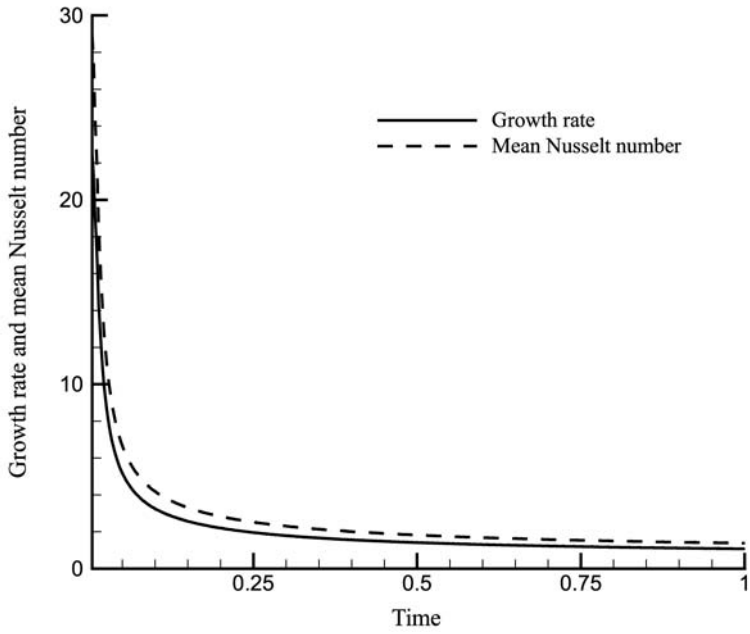

Figure 3.
Bubble volume growth rate and mean Nusselt number versus time

Figure 3 shows the growth rate of bubble volume and mean Nusselt number changing with dimensionless time at (Re, We) = (2,20). As $Re = 2$ and the term of $Ja/RePr$ on the right hand side of equation (13) is almost a constant for given bulk liquid, so that the growth rate and mean Nusselt number have almost the same magnitude for the whole process of bubble growth. Moreover, as the temperature gradient is higher at initial stage of growth than at the intermediate and final stages, the rates of bubble growth and heat transfer are the highest at the initial stage. Figures 4(a) and (b), respectively, show the relations between the growth rate and mean Nusselt number at different Re and We. At higher Reynolds number, the magnitude of bubble growth rate is different from that of mean Nusselt number; with time marching, the mean Nusselt number increases with Reynolds number, but the growth rate does not.

Bubble growth and deformation

Figure 5 shows the results of vapour bubble growth and deformation. At the initial stage, the bubble tries to keep its initial shape (in the present calculation, the initial bubble is assumed to be spherical, as it is simple). By reaching to the intermediate stage, the bubble deformation starts to take place; this is greatly dependent on the terminal value of Reynolds and Weber numbers. At low Reynolds number and relatively large Weber number, as shown in Figure 5(a) (Re, We) = (2,20), the bubble almost maintains its initial shape of spherical without a notable deformation (except the volume increase) until the computational terminal state. In such a situation, the bubble growth may actually play the same role as the surface tension force, which makes the bubble tend to be its initial shape of spherical. With increasing of Reynolds number and decreasing of Weber number, as shown in Figures 5(b) and (c), the bubble

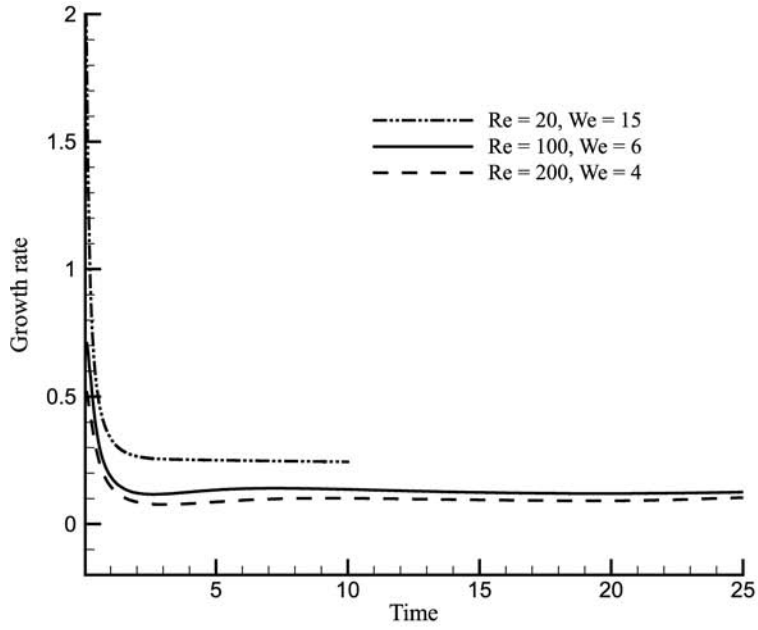

(a) Bubble growth rate versus time for different Reynolds and Weber numbers

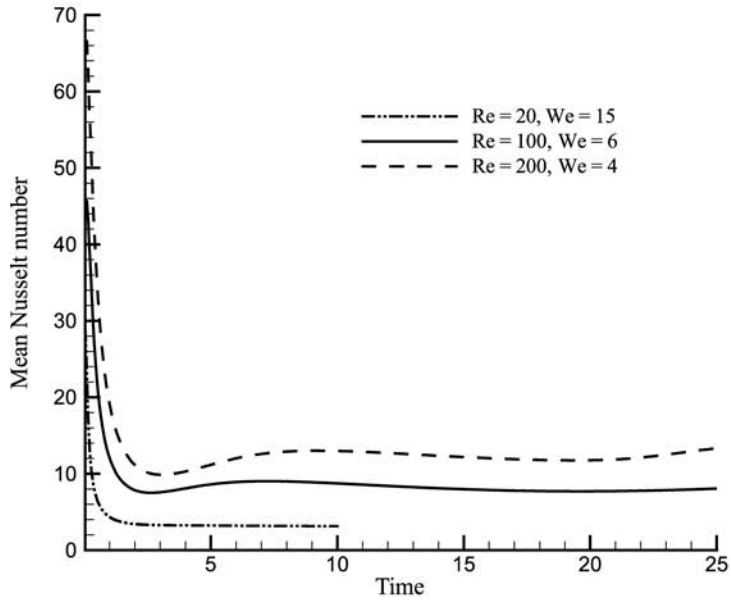

(b) Mean Nusselt number at bubble interface versus time (dimensionless)

Figure 4.

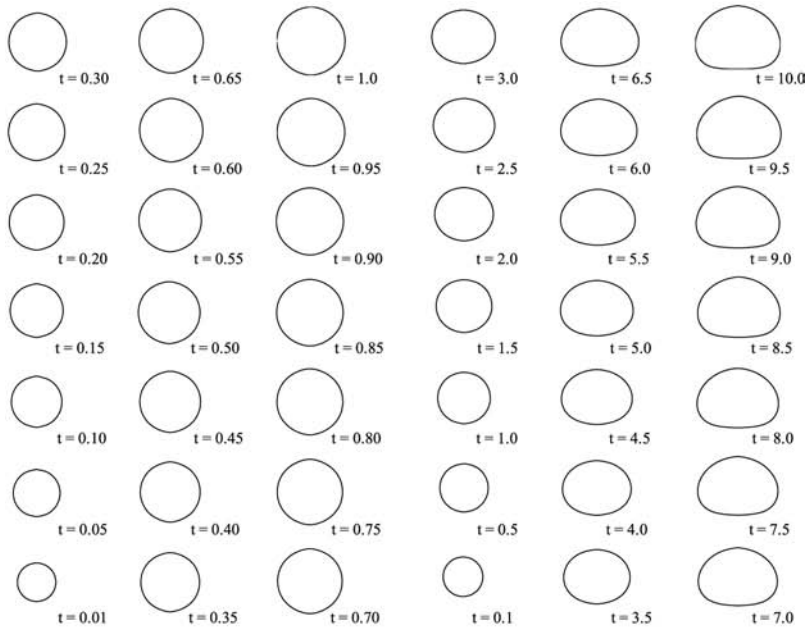

(a) Bubble shape at $Re = 2$ and $We = 20$

(b) Bubble shape at $Re = 20$ and $We = 15$

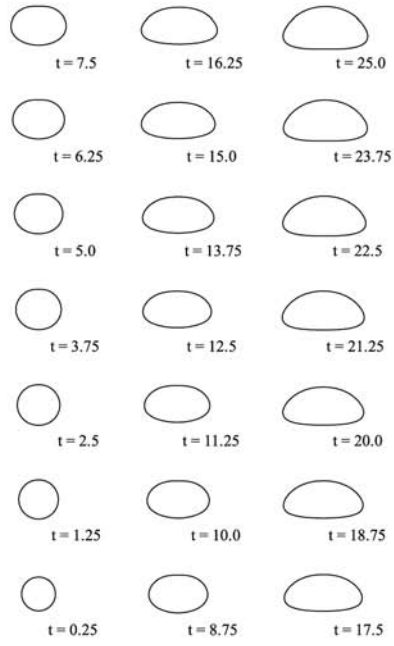

(c) at $Re = 200$ and $We = 4$

Figure 5.
Evolution of bubble shape

experiences a larger deformation at the intermediate and final stages; this indicates that the inertia forces at the interface are larger than the sum of the surface tension and growth forces. Typically, at high Reynolds number, the path of bubble growth and deformation is from a spherical to a fore-flatted and aft-spherical dimpled at intermediate stages, and then it change its shape from a fore-flatted and aft spherical to a fore-spherical and aft-flatted dimpled, as shown in Figure 5(c).

A comparison is made to show the difference between a vapour bubble and a same sized inert bubble (Li *et al.*, 2003). At the same Reynolds and Weber numbers, Figure 6 shows the evolution of these two types of bubbles, respectively; significant differences can be identified. The terminal steady shape of the inert bubble is a dimpled at $t = 4.5$, looks like a crescent, while the vapour bubble with growth is an ellipsoidal at the same dimensionless time. With time marching, the shape of the vapour bubble becomes fore-spherical and aft-flattered ellipsoidal.

Propagation of temperature field

Figure 7 shows the propagation of temperature fields in the vicinity of growing and deformed bubbles. The propagation of temperatures is mainly dependent on the bubble growth and deformation. At low ratio of Reynolds number to Weber number, as shown in Figure 7(a), the effect of convection on the temperature field is weaker than diffusion so that the field is nearly uniform around the bubble; but the distribution is significantly inhomogeneous at the front and rear stagnant points. This is because the non-uniform bubble growth results in an inhomogeneous outwards normal velocity at the interface, and the inhomogeneity decreases with time. Typically, the temperature contours are not parallel with the interfacial outline at initial stages of bubble deformation; as the bubble growing and deforming, the temperature wake does not appear in the rear of the bubble.

At a high ratio of Reynolds and Weber numbers, the convection becomes stronger so that the temperature wake is formed behind the bubble. Figure 7(b) shows the propagation of temperature at $(Re, We) = (20,15)$, and Figure 7(c) shows the case at $(Re, We) = (200,4)$. It is seen that the temperature wake not only changes with Reynolds and Weber numbers but also changes with time. It is notable that at a certain ratio of Re/We, with time marching, the volume of the wake becomes bigger and bigger. With a larger ratio of Re/We, the bubble takes longer to reach its terminal shape.

Conclusions

In this paper, a numerical procedure is proposed to determine improved positions of the bubble-liquid interface at each time step with a whole iteration. Using the code and the methods developed in the present study, a complete numerical solution is obtained for

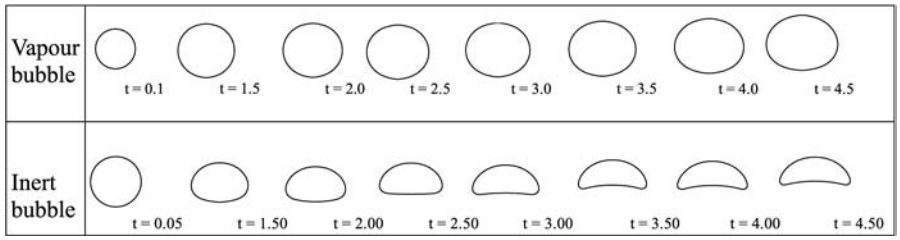

Figure 6.
A comparison of evolution of bubble shape at $Re = 20$ and $We = 15$

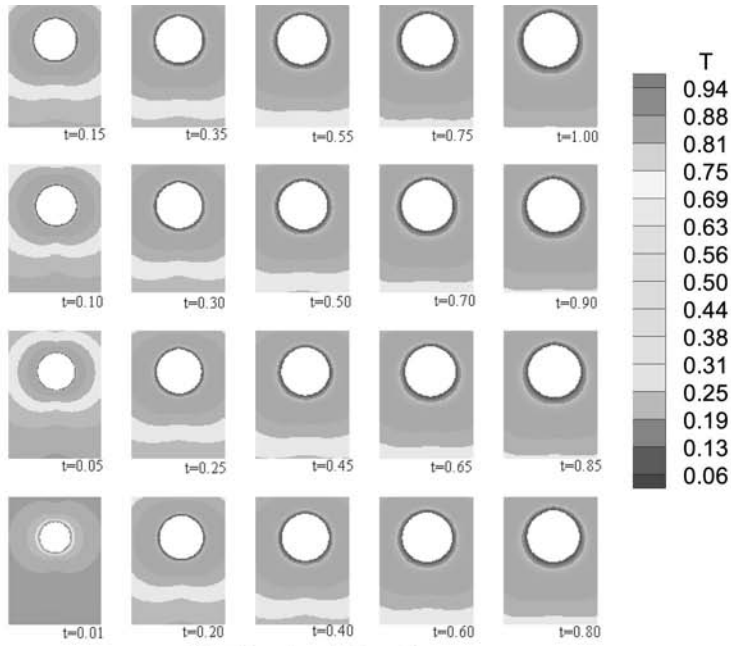

(a) at $Re = 2$ and $We = 20$

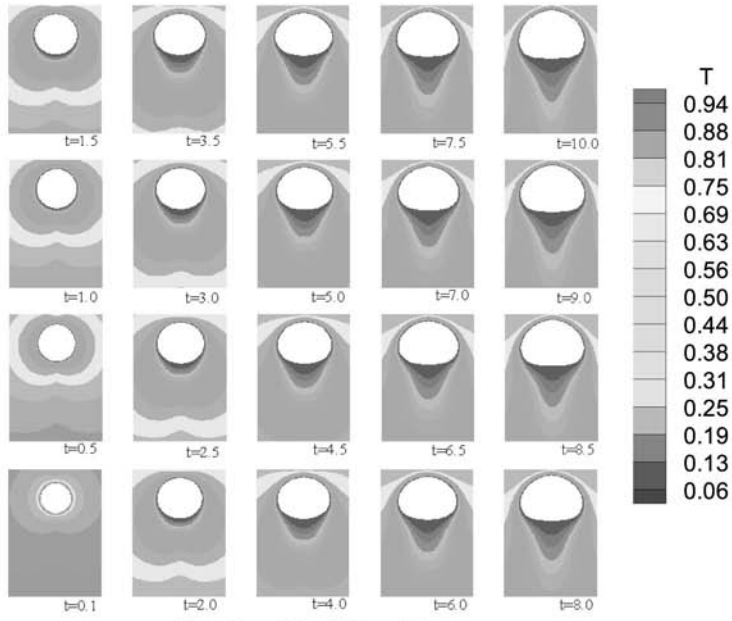

(b) at $Re = 20$ and $We = 15$

(*continued*)

Figure 7.
Propagation of temperature fields

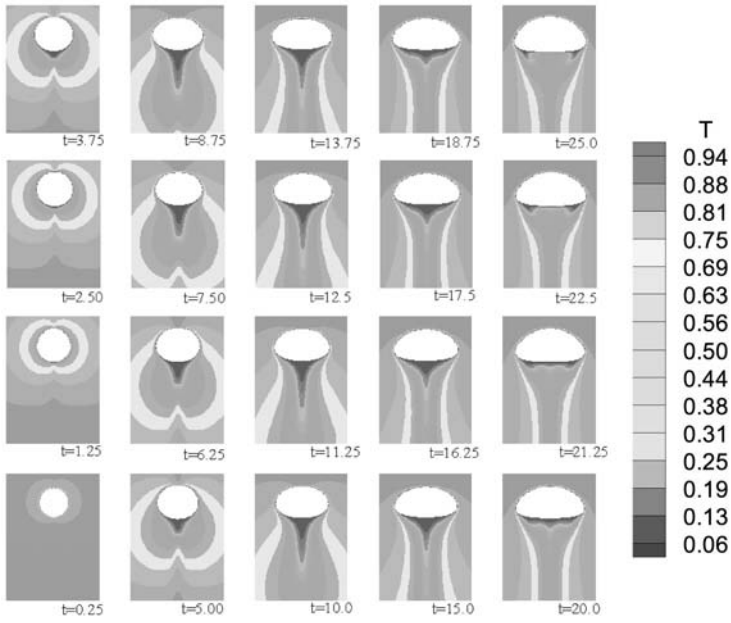

(c) at $Re = 200$ and $We = 4$

Figure 7.

the growth and deformation of a vapour bubble in superheated liquid, this can be summarised as follows:

(1) he rate of vapour bubble growth and the mean Nusselt number change with time; they are the maximum at the initial stage, and then decrease until a certain value.

(2) The rate of bubble growth and the mean Nusselt number are dependent on Reynolds and Weber numbers. The growth rate is inverse proportional to the ratio of Reynolds to Weber numbers, while the mean Nusselt number is proportional to the ratio.

(3) The growth and deformation of vapour bubble at different ratios of Re/We are calculated. The results show that, at the initial stage of evolution, the bubble tends to be its initial shape, but the changes in shape are quite different at the intermediate stages of evolution in particular at high ratio of Re/We.

(4) The rate of bubble growth has a significant effect on the bubble deformation. The growth makes the bubble tend to be its initial shape such as spherical.

(5) The vapour bubble growth and deformation have a great influence on the propagation of temperature fields. The temperature wake behind the bubble does not appear at low Reynolds number, but it occurs at high Reynolds number.

References

Buyevich, Y.A. and Webbon, B.W. (1996), "Dynamics of vapour bubbles in nucleate boiling", Vol. 39 No. 12, pp. 2409-26.

Cao, J. and Christensen, R.N. (2000), "Analysis of moving boundary problem for bubble collapse in binary solutions", *Numerical Heat Transfer, Part A*, Vol. 38, pp. 681-99.

Clift, R., Grace, J.R. and Weber, M.E. (1978), *Bubbles, Drops, and Particle*, Academic Press, New York, NY, pp. 23-8.

Demirdzic, I. and Peric, M. (1988), "Space conservation law in finite volume calculations of fluid flow", *Int. J. Numer. Methods Fluids*, Vol. 8, pp. 1037-50.

Fujita, Y. and Bai, Q. (1998), "Numerical simulation of the growth for an isolated bubble in nucleate boiling", *Proceedings of 11th IHTC, Kyongiu, Korea, August 23-28*, Vol. 2, pp. 437-42.

Han, Y.Y. and Seiichi, K.Y.O. (2001), "Direct calculation of bubble growth, departure, and rise in nucleate pool boiling", *Int. J. of Multiphase Flow*, Vol. 27, pp. 277-98.

Li, W.Z. and Yan, Y.Y. (2002a), "An alternating dependent variables (ADV) method for treating slip boundary condition of free surface flows with heat and mass transfer", *Numerical Heat Transfer*, Vol. 41 No. 2, pp. 165-89.

Li, W.Z. and Yan, Y.Y. (2002b), "Direct-predictor method for solving steady terminal shape of a gas bubble rising through a quiescent liquid", *Numerical Heat Transfer*, Vol. 42 No. 1, pp. 55-71.

Li, W.Z., Yan, Y.Y. and Hull, J.B. (2003), "The propagation of temperature and concentration fields around a deformed gas bubble rising in a quiescent hot or bi-solution liquid", *Int. J. of Numerical Methods for Heat & Fluid Flow*, Vol. 12 No. 8, pp. 940-63.

Magnaudet, J. and Eames, I. (2000), "The motion of high-Reynolds-Number bubbles in inhomogeneous flows Magnaudet", *Annual Review of Fluid Mechanics*, Vol. 32, pp. 659-708.

Mei, R., Chen, W. and Clausner, J. (1995a), "Vapour bubble growth in heterogeneous boiling – I", *Formulation*, Vol. 38 No. 5, pp. 909-19.

Mei, R., Chen, W. and Clausner, J. (1995b), "Vapour bubble growth in heterogeneous boiling – II", *Formulation*, Vol. 38 No. 5, pp. 921-34.

Patankar, S.V. (1980), *Numerical Heat Transfer and Fluid Flow*, Hemisphere Publications corporation, New York, NY.

Plesset, M.S. and Zwick, S.A. (1953), "The growth of vapour bubble in superheated liquids", *J. of Applied Physics*, Vol. 25 No. 4, pp. 293-500.

Son, G. and Dhir, V.K. (1998), "Numerical simulation of a single bubble during partial nucleate boiling on a horizontal surface", *Proceedings of 11th IHTC, Kyongiu, Korea, August 23-28*,Vol. 2, pp. 533-8.

Wittake, D.D. and Chao, T.B. (1967), "Collapse of vapour bubbles with translatory motion", *J. Heat Transfer*, Vol. 89, pp. 17-24.

Yan, Y.Y. and Li, W.Z. (2002), "Numerical investigations of the flow and heat and mass transfer at the surface of a spherical gas bubble", *Int. J. Transport Phenomena*, Vol. 4 No. 3, pp. 209-24.

Yan, Y.Y., Li, W.Z. and Smith, J.M. (2002), "Numerical simulation of the behaviour of a single deformable bubble in two-phase flow", *Proceedings of 12th International Heat Transfer Conference, Grenoble, France, 18-22 August*,Vol. 3, pp. 575-80.

Corresponding author
Y.Y. Yan can be contacted at: yuying.yan@nottingham.ac.uk

To purchase reprints of this article please e-mail: **reprints@emeraldinsight.com**
Or visit our web site for further details: **www.emeraldinsight.com/reprints**